Appl Phys B (2008) 92: 623–626
DOI 10.1007/s00340-008-3141-0

Applied Physics B
Lasers and Optics

Directional terahertz radiation through groove-assisted hole array

Y. Liu · H. Shi · J. Ma · D. Gan · J. Cui · C. Du · X. Luo

Received: 20 February 2008 / Revised version: 4 June 2008 / Published online: 8 August 2008

Abstract The authors theoretically demonstrate the terahertz beam shaping with metallic subwavelength holes array surrounded by concentric periodic grooves. High transmission and directional radiation can be obtained simultaneously for the resonant excitation of the surface wave in the combined structure. Finite-difference time-domain simulation results shows that the transmission mainly depends on the lattice constant of hole array and the features of incident surface around it, while the far-field angle distribution is dominated by the details of the output surface. This compact beam shaping structure is hoped to serve as a basic device for future terahertz systems.

PACS 77.65.Dq · 95.85.Gn · 41.85.Ct · 42.25.Bs

1 Introduction

Recently, with rapid development of terahertz (THz) source and detector technology, THz technical benefits are promising for applications in medical imaging, security scanning, and communications [1–3]. This trend requires the tremendous progress of beam shaping devices integrated into the THz systems. The polypropylene diffractive optical elements operated at THz frequency were proposed and fabricated to fulfill this end [4]. However, the fabrication process of the diffractive optical elements needs multialignment etching for its multiple-phase level. On the other hand, the recent appearance of surface plasma subwavelength optics (SPSO) opens a previously inaccessible pathway for the development of the compact THz devices with structured metallic films [5–7]. It has been successfully demonstrated in the THz region that the two-dimensional (2D) metallic hole array could serve as an effective band pass filter [8–10]. And subwavelength grooves patterned on the exit plane of metallic film deliver manipulation of light in nanodimensions and reduced diffraction in the far field [11–13]. Special metallic bow-tie shaped aperture surrounded by periodical corrugations could achieve subwavelength resolution imaging in the near-field region [14]. In this letter we propose a compact metallic THz beam shaping element with subwavelength hole array surrounded by concentric periodical grooves, which can focus the THz wave and obtain high transmission simultaneously. This makes it an excellent candidate for various compact THz beam shaping applications.

2 Numerical simulation and discussion

Figures 1a and b illustrate the schematic view of the proposed THz beam shaping structure. The $n \times n$ rectangular hole array surrounded by several concentric periodic grooves are formed in a freestanding metallic film, and the circular grooves are placed on both the input and the output surfaces. The film thickness is h, the hole dimensions are $l \times w$, the lattice constant of hole array is p, the groove period is b, the groove width is $b/2$, the groove depth is a, and

Y. Liu · H. Shi · D. Gan · J. Cui · C. Du (✉) · X. Luo
State Key Lab of Optical Technologies for Microfabrication, Institute of Optics and Electronics, Chinese Academy of Sciences, Chengdu 610209, China
e-mail: cldu@ioe.ac.cn

X. Luo
e-mail: lxg@ioe.ac.cn

J. Ma
College of Information Engineering, Shenzhen University, Shenzhen 518060, China

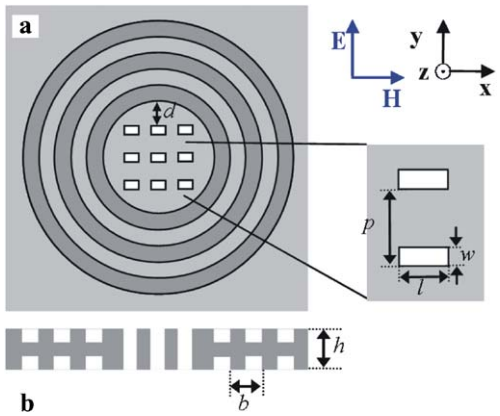

Fig. 1 Schematic illustration of hole array surrounded by concentric periodic grooves. (**a**) Top view of the structure; (**b**) side cross-sectional view of the structure

the distance from the edge of the hole array to the nearest groove along y-axis is d.

Two conditions must be satisfied in order to achieve the combination of the extraordinary transmission effect of the hole array and the beaming effect of the concentric periodic grooves sufficiently. First, the peak of transmission spectra for hole array and the concentric periodic grooves need to coincide with each other. Second, hole array and grooves should be in proper relative position to make sure that the coupling between them is strongest. The geometric factors play a critical role in this effect. Hence, we set the lattice constant of hole array at $p = 170$ μm. Length, width of holes, the film thickness, the groove depth, and groove period, is $l = 92$ μm, $w = 50$ μm, $h = 60$ μm, $a = 20$ μm, and the $b = 186$ μm, respectively. If the number of holes is large enough, the transmission of hole array is high and sufficient for various practical applications. Here we took a simple case of 3×3 hole array with the purpose to illustrate this phenomenon. The number of concentric periodic grooves is 6 and the radius of the inner groove is 350 μm.

Figure 2 presents the calculated transmission spectra for the single subwavelength aperture, the 3×3 hole array, and the hole array with concentric periodic grooves only in incident surface and in both surfaces, respectively. Three-dimensional finite-difference time-domain (FDTD) method is employed with the perfectly matched layer absorbing boundary condition. The dimensions of each grid cell are $\Delta x = \Delta y = 10$ μm, $\Delta z = 4$ μm, and the time step is set as $\Delta t = 6.79\text{E}{-}15$ s. The metal is assumed to be the perfect conductor, which makes an excellent approximation in the THz range. The plane wave with the electric field polarized in the y direction impinges on the structure at normal incidence. From the results shown in Fig. 2a, it can be seen that for a single 92×50 μm aperture, the transmission is very low. A resonant transmission peak appears for 3×3 hole array structure at 198 μm wavelength, which

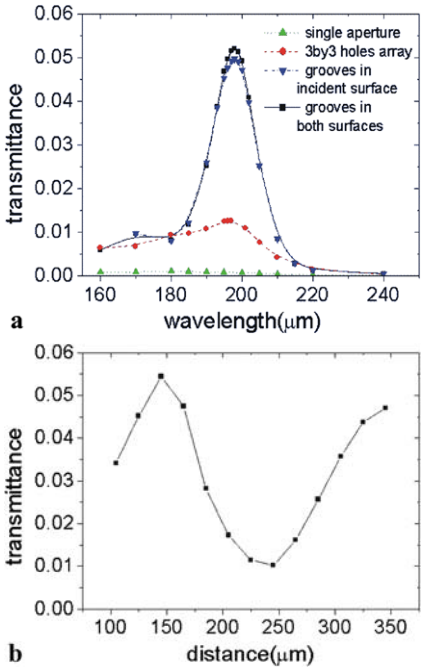

Fig. 2 (**a**) Calculated transmission spectra for a single subwavelength aperture 92×50 μm (*green*), 3×3 hole array (*red*) and hole array with concentric periodic grooves in the incident surface (*blue*) and both surfaces (*black*). (**b**) Calculated transmission versus distance d. The incident light THz wave is y-polarized with a wavelength of 198 μm

is close to the periodicity of the concentric grooves. The structure with the concentric periodic grooves provided a nearly fivefold enhancement in peak transmission in comparison to the case without the concentric periodic grooves while the peak wavelength is constant. Here, the transmittance is about 5.2%, which means that the normalized to the area transmittance excesses 11, and a further enhancement of the transmission can be expected by increasing the number of the holes. The transmission spectra for the cases with grooves corrugated in the incident surface and both surfaces are nearly identical. The reasons for the above phenomenon may be explained as follows. For a single subwavelength aperture, the cutoff wavelength of the subwavelength aperture is shorter than the incident wavelength, so only little THz wave can get through. For the subwavelength hole-based array, not only the transparent area increases, but also the coupling between the holes plays an important role for the enhanced transmission in the case of phase matching condition: wavelength of the incident wave is slightly longer than the period of hole array [15]. It is worth to note in Fig. 2a that only the grooves in the incident surface make effect to enhance the transmission. The incident THz wave at wavelength close to the periodicity of concentric grooves can be converted to the surface mode, which is due to resonant coupling caused by the periodic grooves in the incident surface. The generated surface waves propagate in the plane and build up a standing wave, which form high-energy den-

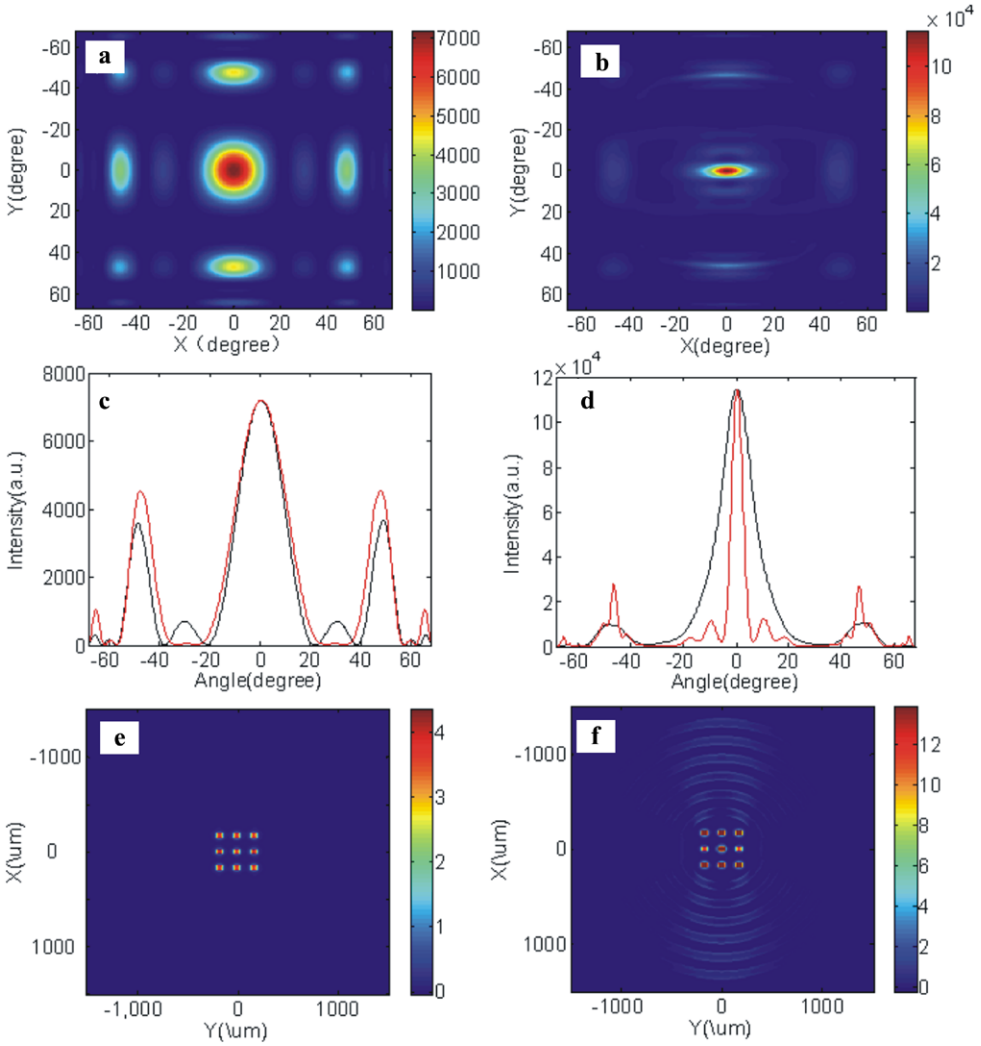

Fig. 3 FDTD simulation results of two-dimensional (2D) intensity distribution $|E_y|^2$ of in far field of (**a**) the 3×3 hole array and (**b**) the holes array with grooves, y-polarized plane wave at $\lambda = 198$ μm is incident to the z-direction. (**c**) and (**d**) are far-field distributions at centric cross-sections alone E (*red color*) and H (*black color*) direction of incident light. (**e**) and (**f**) are time-averaged E_y-field energy densities in the exit plane at 4 μm distance from exit surface of the 3×3 hole array and the hole array with grooves, respectively

sity of the surface mode located in the hole array. Consequently, the introduction of the circular grooves in the incident surface results in a further increase of the transmission enhancement.

The relative position of hole array and concentric periodic grooves can effectively control the enhanced transmission phenomenon. Figure 2b shows the transmission versus distance d for incident wavelength $\lambda = 198$ μm, the maximum transmission happens when $d = 3/4\lambda$, as the effective coupling between the hole array and the grooves is strongest. In the case of $d = 5/4\lambda$, the transmission is lowest and equals to that of the 3×3 hole array, which means that there is no effective coupling. By varying the distance d, we can modulate the transmission periodically. The period is about 200 μm and is approximately equal to the wavelength of the surface wave since λ_{sp} is approximately equal to λ.

Figure 3 presents the calculated $|E_y|^2$ distribution of the 3×3 hole array with and without periodic grooves in both near field and far field. The normal incident wave is y-polarized at the wavelength of 198 μm. Figure 3a shows the far-field intensity distribution of the hole array. There are nine lobes totally. Figure 3c shows the far-field intensity distribution at the centric cross-section of Fig. 3a along E and H direction of the incident wave. It can be seen that two curves are nearly identical and the centric lobe concentrates most energy. The full width at half maximum (FWHM) at the central lobe along E and H directions are 22.48° and 20.52°, respectively. The maximum intensities of the side lobes proportional to the central spot along E and H directions at 62.3% and 50.0%, respectively. Figures 3b and d show the 2D far-field intensity distribution of the hole array with grooves and its centric cross-sections along E and H direction. The intensity of side lobes are greatly suppressed, only the main lobe which concentrates most of energy appeared in the center of the far field. The maximum intensity which is 16 times greater than that of the 3×3 hole array. The most interesting phenomenon is that the corresponding FWHM along the E direction is only 4.95°, meaning that just only about 1/5 of the one with bare array. The FWHM along the H direction is 14.56°, about 2/3 of the previous

case. The maximum intensities of side lobe along both E and H directions are 24.4 and 8.9%, respectively. This result indicates that the concentric periodic grooves suppress the side lobe and greatly reduce the size of the central light spot in far-field region.

The grooves on the output surface are responsible for the beaming effect of the THz wave. The excitation of surface mode causes the high-field enhancement in the grooves around the holes, whereby each groove reradiates power and can be considered as secondary source. It is the in-phase coupling between these secondary sources and primary source (the hole array) that results in the strong angular confinement and directivity of the transmitted THz wave. Therefore, the intensity of side lobe is suppressed and the size of the main lobe becomes smaller. However, the high-field enhancement only occurs in the area parallel to the hole array along the E direction, as shown in Figs. 3e and f. Thus the centric angular lobe is greatly suppressed along the E direction compared to that of the H direction.

This combined structure of hole array and concentric periodic grooves which can focus the THz wave can be employed as a THz device used in the future THz wave-related systems. Transmission and far-field divergence angle can be modulated respectively by these structures. The former is determined by geometrical parameters of the hole array and grooves at the incident plane, and the latter is controlled by the grooves at the exit plane. Design freedom of the THz devices is greatly improved accordingly. Although this device can not create arbitrary energy distribution in the far field, it is a helpful attempt for the development of subwavelength metallic THz device with much smaller size compared to traditional cylindrical lens and can be easily integrated with other THz devices and systems.

3 Summary

In summary, we designed a novel structure of groove-assisted hole array which can serve as a THz beam shaping device. The FDTD (finite-difference time-domain) simulations demonstrate that the coincidence of both peak wavelengths of the hole array and the concentric periodic grooves leads to large enhanced transmission and beaming effect. The transmission and the far-field distribution of the structures can be modified by simply tuning geometrical parameters of the structures, which make such structures excellent candidates for the compact THz-related beam shaping devices.

Acknowledgements This work was supported by 973 Program of China (No. 2006CB302900) and National Natural Science Foundation of China (No. 60778018).

References

1. B.B. Hu, M.C. Nuss, Opt. Lett. **20**, 1716 (1995)
2. D.L. Woolard, E.R. Brown, M. Pepper, M. Kemp, Proc. IEEE **93**, 1722 (2005)
3. M.M. Awad, R.A. Cheville, Appl. Phys. Lett. **86**, 221107 (2005)
4. E.D. Walsby, J. Alton, C. Worrall, H.E. Beere, D.A. Ritchie, D.R.S. Cumming, Opt. Lett. **32**, 1141 (2007)
5. J.B. Pendry, L. Martin-Moreno, F.J. Garcia-Vidal, Science **305**, 847 (2004)
6. A.P. Hibbins, B.R. Evans, J.R. Sambles, Science **308**, 670 (2005)
7. S.A. Maier, S.R. Andrews, L. Martin-Moreno, F.J. Garcia-Vidal, Phys. Rev. Lett. **97**, 176805 (2006)
8. H. Cao, A. Nahata, Opt. Express **12**, 3664 (2004)
9. D. Qu, D. Grischkowsky, W. Zhang, Opt. Lett. **29**, 896 (2004)
10. J.W. Lee, M.A. Seo, D.J. Park, D.S. Kim, S.C. Jeoung, Ch. Lienau, Q.-H. Park, P.C.M. Planken, Opt. Express **14**, 1253 (2006)
11. C. Wang, C. Du, Y. Lv, X. Luo, Opt. Express **14**, 5671 (2006)
12. H. Shi, C. Du, X. Luo, Appl. Phys. Lett. **91**, 093111 (2007)
13. Y. Liu, H. Shi, C. Wang, C. Du, X. Luo, Opt. Express **16**, 4487 (2008)
14. K. Ishihara, K. Ohashi, T. Ikari, H. Minamide, H. Yokoyama, J. Shikata, H. Ito, Appl. Phys. Lett. **89**, 201120 (2006)
15. J.B. Abad, A. Degiron, F. Przybilla, C. Genet, F.J. Garcia-Vidal, L. Martin-Moreno, T.W. Ebbesen, Nature Phys. **2**, 120 (2006)